Tutor/s

Dra. Maria Sarret Pons
Departament de Ciència dels Materials i Química Física

Dr. Aldo Roda
Università di Bologna

Grau de Química

Treball Final de Grau

Chemiluminescent bioanalytical assays for clinical biomarkers.

Assajos bioanalítics quimioluminescents per biomarcadors clínics.

Guillem Campmajó Galván

June 2017

Universitat de Barcelona

B:KC Barcelona Knowledge Campus
Campus d'Excel·lència Internacional

El meu agraïment al Prof. Aldo Roda i a la Prof. Mara Mirasoli per brindar-me l'oportunitat de realitzar aquest treball al grup d'investigació de Química Analítica i Bioanalítica de l'Università di Bologna i per l'ajut en la realització d'aquest estudi. També, la meva gratitud a la Dra. Martina Zangheri i al Dr. Donato Calabria pel seu recolzament diari, el seu consell i la seva dedicació.

També, donar les gràcies a la Dra. Maria Sarret pel seu suport i la seva guia malgrat la distància.

Finalment, agraeixo a tots els integrants del laboratori haver-me fet sentir com a casa i fer d'aquesta, una experiència que difícilment oblidaré.

REPORT

CONTENTS

1. SUMMARY

A growing field of research in chemical-biological analysis, aimed at improving and simplifying analytical procedures, is the development of Lab-On-Chip devices. Allowing the direct analysis at the point of need, the use of such portable miniaturized systems offers many applications ranging from environmental analysis to complementary diagnostics for personalized medicine. Moreover, due to its numerous advantages over traditional photon emission detection techniques, chemiluminescence has proven to be suitable for that type of devices.

This study has been focused on the development of two chemiluminescent bioanalytical assays for clinical biomarkers. In particular, the optimization of bioanalytical assays required the study of different materials and procedures for obtaining optimal performances, with special attention to the development of suitable immobilization procedures and to the selection of proper reagents, materials and chemiluminescent detectors.

On one hand, a chemiluminescent immunoassay for detection of ATP has been optimized. Among three different immunoassay formats, the indirect competitive immunoassay based on the immobilization of ATP conjugated to ovalbumin was selected as the most appropriate. After its optimization in 96-microwells platform, a calibration curve was obtained.

On the other hand, a “paper-based” analytical device, which exploits an enzymatic reaction for quantification of glucose in serum sample, has been adapted from a CCD camera to a more compact and portable CMOS sensor for the detection. In result, the adaptation was successfully achieved without a significant loss in detectability.

Keywords: Chemiluminescence, Lab-On-Chip, bioassays, immunoassay, enzymatic assay, paper-based device, CMOS sensor, ATP, glucose, biomarker.

2. RESUM

Un camp d'investigació en creixement en anàlisi química-biològica, dirigit a millorar i simplificar els procediments analítics, és el desenvolupament dels dispositius "Lab-On-Chip". Permetent l'anàlisi directa en el punt de necessitat, l'ús d'aquests sistemes portàtils miniaturitzats ofereix un ampli rang d'aplicacions que van des d'anàlisis mediambientals fins al diagnòstic complementari per la medicina personalitzada. A més, degut a les seves nombroses avantatges respecte les tècniques clàssiques de detecció d'emissió de fotons, la quimioluminescència ha demostrat ser una tècnica convenient per a aquest tipus de dispositius.

Aquest estudi s'ha basat en el desenvolupament de dos assajos bioanalítics quimioluminescents per biomarcadors clínics. En particular, l'optimització dels assajos bioanalítics ha requerit l'estudi de diferents materials i procediments per a l'obtenció de resultats òptims, amb especial atenció en el desenvolupament dels procediments d'immobilització adequats i en la selecció apropiada dels reactius, materials i de la detecció quimioluminescent.

Per una banda, un immunoassaig quimioluminescent per a la detecció d'ATP ha estat optimitzat. D'entre tres formats d'immunoassaig, un immunoassaig competitiu indirecte basat en la immobilització d'ATP conjugat a ovoalbúmina va ser triat com el més adequat. Després de la seva optimització en microplaca com a plataforma, es va obtenir una corba de calibratge.

D'altra banda, un dispositiu analític basat en paper, que empra una reacció enzimàtica per a la quantificació de glucosa en una mostra de sèrum, s'ha adaptat d'una càmera CCD ultrasensible a un sensor CMOS, més compacte i portàtil, com a detector. A partir dels resultats obtinguts, es va demostrar que l'adaptació es va aconseguir de forma exitosa sense una pèrdua significativa en la detectabilitat.

Paraules clau: Quimioluminescència, "Lab-On-Chip", bioassajos, immunoassaig, assaig enzimàtic, dispositiu basat en paper, sensor CMOS, ATP, glucosa, biomarcador.

3. INTRODUCTION

3.1. POINT-OF-CARE TESTING DEVICES

In the last years, one of the main issues in the field of Analytical Chemistry has been the development of analytical systems capable of providing fast and reliable analytical results exploiting easy-to-use and portable devices suitable for performing the analysis directly at the point of need. In diagnostic field this approach is known as "Point-of-care testing" (POCT) and it must meet the following basic requirements [1]:

- The sample has to require a minimum or nil pre-treatment before the analysis.
- Structural characteristics as small size, reduced weigh and the presence of an autonomous electrical power should ensure the portability of the device.
- People without knowledge in the field are supposed to use the system, so it has to be user-friendly.
- Qualitative or quantitative results, depending on the objective of the analysis, must be obtained by treating the primary measurement output provided by the detection system.

In addition, POCT devices should be based on low cost and disposable components and it should guarantee stability and durability from the fabrication to their use. Other important characteristics of POCT systems are the possibility to automate the analytical process, to have an internal control for the auto-calibration, to provide a wide measurement range or the ability to determinate multiple analytes simultaneously.

3.2. LUMINESCENCE AND CHEMILUMINESCENCE

3.2.1. Luminescence's processes. Chemiluminescence

Luminescence consists in the emission of electromagnetic radiation in the UV-Vis region (200-800 nm), due to molecules or atoms, as a result of a transition from an excited electronic state to a state with a lower energy, normally the ground state.

Different forms of luminescence are classified depending on the origin of the photon's production. Thus, for example, a physic stimulus as electromagnetic radiation can produce fluorescence or phosphorescence, while, chemical luminescence is caused by a chemical reaction.

According to the stimulus able to trigger the reaction, chemical luminescence can be classified in different subtypes: chemiluminescence (CL) and bioluminescence are referred to the chemical production of light started by mixing the reagents and, in case of BL, using enzymes and photoproteins isolated from living organisms [2]; in electrogenerated chemiluminescence, reagents are produced during an electrochemical reaction that occurs at the surface of an electrode and the light is generated by the relaxation of that molecules [3]; in thermochemiluminescence the light is produced by the thermal-induced decomposition of a molecule [4].

A chemical reaction produces light when it fulfils some specific requirements [5]:

- The reaction needs to be exergonic enough to populate an electronically excited singlet state. The emission of photons in the region between 400 and 750 nm requires an energy of 40-70 $kcal \cdot mol^{-1}$
- The excited state's formation has to be accessible respect the ground state on the reaction coordinate.
- To carry out the photon emission, the release of energy has to be feasible. In direct CL, the excited molecule responsible of the light is produced by the chemical reaction, whereas, in indirect CL, the reaction produces an excited compound, which cannot release light, but transfers that energy to a molecule that can, as shown in Figure 3.1.

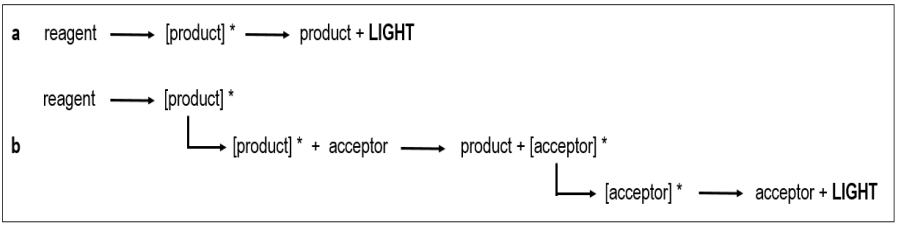

Figure 3.1 *Direct (a) and indirect (b) CL reaction.*

3.2.2. Chemiluminescent quantum yield

The capacity of the CL system to emit light is expressed by the CL quantum yield (Φ_{CL}), defined as the number of photons emitted per reacting molecule and represented by the expression:

$$\Phi_{CL} = \Phi_R \Phi_{ES} \Phi_F$$

where Φ_R is the chemical yield of the reaction, Φ_{ES} is the fraction of molecules that arrived at the excited state and Φ_F is the fraction of molecules that returns to the ground state by releasing photons. In indirect CL reactions, $\Phi_{ET,}$ which is the process of energy transfer, should be added. Normally, a CL reaction has a value of the CL quantum yield between 0'001 and 0'1. There are different factors that influence that value: the intrinsic luminescent power of the excited molecule, the pH, the temperature or the concentration of the reagents.

3.2.3. Chemiluminescent detection

CL analytical techniques have achieved great popularity in the recent years thanks to their ability to produce photons with no need for photoexcitation, as it occurs in fluorescence detection, thereby avoiding problems arising from light scattering, background fluorescence or light source instability. CL detection techniques are characterised by a high signal-to-noise ratio, hence a high sensitivity, as the light signal is generated by the chemical reaction in the dark. CL-based detection is particularly suited for miniaturized analytical devices, as it avoids the need for external radiation sources and complex optical systems combining filters and lenses [6]. Moreover, CL detection shows wide dynamic ranges, thus facilitating analysis of samples with very different analyte concentrations.

In contrast to other spectroscopic techniques, the CL signal is not constant. However, it presents a kinetic that depends on the reaction rate, which decreases over time. Figure 3.2 shows two kind of signals that can be produced by a CL reaction: flash or glow kinetic.

- CL reactions that have a flash kinetic, reach instantly the maximum intensity and the signal decreases exponentially over time. That kinetic is very fast, so it requires an instrumentation able to activate the reaction inside the device ensuring the detection of the signal. Moreover, as the highest intensity of the signal is influenced by different factors (e.g. temperature, pH and presence of

interferents), it is not a reliable data. So, in this case the signal is integrated over a certain time.

- CL reactions that have a glow kinetic are normally catalysed by enzymes. In that case, the emission achieve quickly a constant intensity and is maintained over a relatively long time. When the substrate is in excess, the maximum signal intensity is proportional to the activity of the enzyme which is related to analyte's concentration.

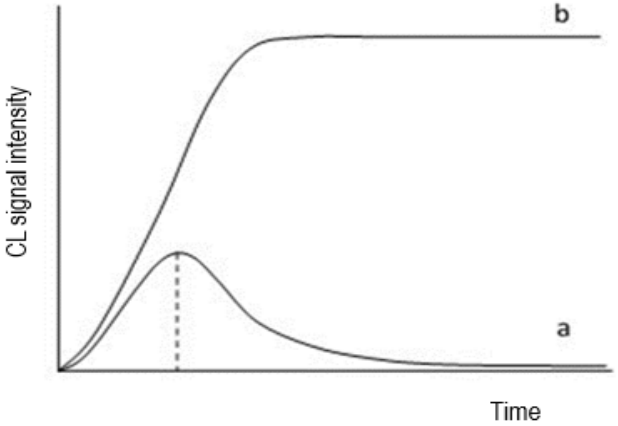

Figure 3.2 *Flash (a) and glow (b) CL reaction kinetics.*

The oxidation of luminol (5-Amino-2,3-dihydrophthalazine-1,4-dione), shown in Figure 3.3, under alkaline conditions in presence of an oxidant agent, as hydrogen peroxide, is one of the most employed CL reactions. Due to the basic pH used, luminol is found as a dianion, which presents keto-imine tautomerization. The disproportionation of hydrogen peroxide produces water and oxygen. That last one, reacts with the imine form of the luminol's dianion producing the excited 3-aminophtalate that when it decays to the ground state, a photon is released emitting at 428 nm (blue light emission).

That reaction can be catalysed by different molecules, from enzymes to metallic coordination complexes. Thus, for example, horseradish peroxidase (HRP) is a type of peroxidase enzyme commonly used as a label in binding assays thanks to its signal amplification capability [7]. Another example is the hexacyanoferrate (III) ion. In that case, a redox reaction is produced between the catalyst, which is reduced, and the hydrogen peroxide

(also luminol can be oxidised due to hexacyanoferrate (III) reduction, but this reaction is rather slower).

Luminol's oxidation allows the determination of the activity of the enzyme used, but also, it is possible to determinate species involved in a reaction able to be coupled to the luminescent one. For example, reactions which produce hydrogen peroxide can be coupled to the CL system (e.g. reactions catalysed by oxidase enzymes).

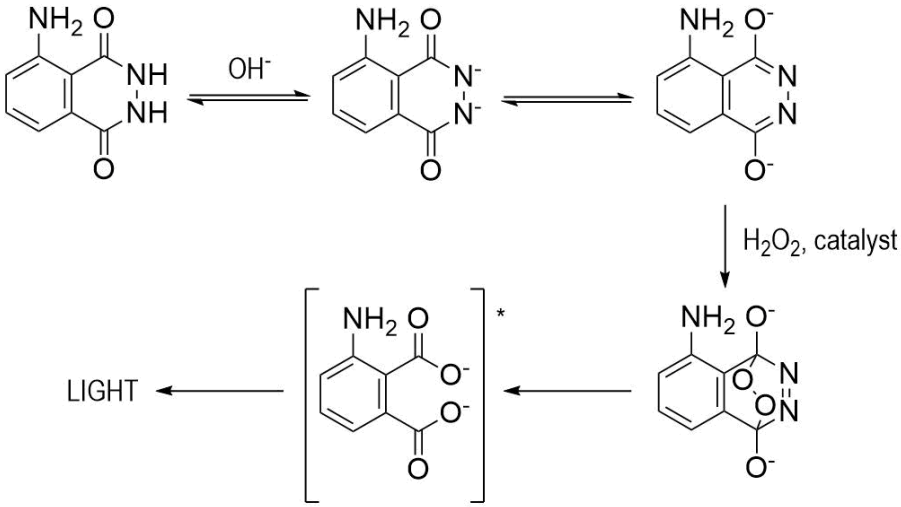

Figure 3.3 *Oxidation reaction of luminol by hydrogen peroxide under alkaline conditions and in presence of a catalyst*

3.2.4. Light detection technologies for biosensing

The main requisite of chemical luminescence measurements is the ability to collect as much light as possible to achieve the highest detectability. In contrast to photoluminescence, where the optics geometry is crucial to minimizing the excited light interference, a much-simplified optics can be used. Several technological solutions have been proposed for ultrasensitive chemical luminescence detection in biosensors and bioassays.

- **Photomultiplier tubes:**

The reference detection system for chemical luminescence is the photomultiplier tube (PMT), which provides the highest sensitivity. Typical PMT devices present a high quantum

efficiency in the spectral range between 360-670 nm, covering the emission wavelengths of the majority of CL probes. Implementation of conventional PMT-based devices in biosensors has been hampered by their high cost, large size, and requirement for a power source.

- **Charge-transfer detectors:**

The requirement for portable light detectors with high sensitivity has led to the use of alternative light sensors, such as charge-coupled devices (CCD), complementary metal oxide semiconductors (CMOS), and silicon and organic photodiodes. Portable charge-transfer detectors (CCD and CMOS) have become widespread thanks to their compact size and their ability to image and quantify multiple spots simultaneously on the detection area of the sensor [8, 9, 10].

The renewed interest in CMOS derives from their small size, low power consumption, camera-on-a-chip integration, and lower fabrication costs [11, 12]. In first generation CMOS, the majority of the pixel area was dedicated to the support transistors, with a limited photon-sensing area (fill factor). Modern back-illuminated CMOS, in which the entire area of each pixel is used for photon capture, offer higher sensitivity, ensuring high signal-to-noise ratio even in low-light conditions. The pixel size is reduced, increasing image resolution and device compactness. Imaging with charge-transfer sensors requires simple optics to obtain reasonable resolution and to prevent light cross-talk between adjacent objects. Alternatively, optics-free “contact imaging” configurations can be used, in which the surface where the bioassays take place is in contact with the sensor [13].

- **Thin-film photosensors:**

The integration of relatively inexpensive thin-film photosensors directly in the analytical chip is another notable technological advance, which could reduce costs, electrical power consumption, and memory storage space. By optimizing chip design, sensor architecture, and readout electronics to maximize photon collection efficiency, analytical performances comparable with CCD have been achieved in a portable integrated device [14].

3.3. BIOSPECIFIC MOLECULAR RECOGNITION

The specific interaction between two or more molecules that exhibit molecular complementarity caused by noncovalent bonding is known as molecular recognition [15]. That noncovalent bonding can be: hydrogen bonding, hydrophobic forces, Van der Waals forces, π-

π interactions, halogen bonding and electrostatic and/or electromagnetic effects. Molecular recognition reactions are widely used in analytical chemistry's field as they are a sensitive and specific biosensing tool.

In spite of the variety of molecular recognition reactions, this work will only focus on immunological and enzymatic methods.

3.3.1. Immunological methods

Immunoassays (IA) are well established bioanalytical methods widely employed for screening procedures offering high sample throughput, high sensitivity and reduced requirements for sample pre-analytical preparation, owing to the high specificity of antigen-antibody binding reaction. Appropriate antibodies bind with high selectivity to their antigen and it is possible to design IA for a wide range of analytes. The antibody is a protein that is able to recognize and bind selectively its own specific antigen by an affinity reaction. The chemical structure of the antigen allows its binding to the paratope of the antibody with high affinity, establishing an equilibrium reaction. This reaction depends on the concentration of the analytes if the antibody and the other reagents are present in constant concentrations. There are a great variety of antibodies that can be raised up for different kind of analytes such as small organic molecules (i.e. pesticides, hormones, pharmaceuticals or toxic small molecules), biopolymers (i.e. peptides, proteins, DNA) or the outer membrane of cells or organelles (i.e. viruses, bacteria, spores, fungi, protozoa, eukaryotic cells), thus allowing the development of rapid and sensitive IA for biological, environmental or food analysis. Monoclonal and polyclonal antibodies are available for IA [16].

The detection of the formed immune-complex is commonly performed through the use of labelled reagents. Enzymes can be chemically coupled to primary detection antibodies, to antigens, to a secondary antibody (which binds to the unlabelled primary antibody), or to streptavidin (which binds to biotinylated antibodies) to obtain enzymatic tracers.

IA can be classified into competitive and non-competitive formats. While in the competitive format an analyte derivative is added and competes with the analyte present in the sample for binding to the antibody, the non-competitive IAs (also known as "sandwich IA") are based on the directly detection of the immune-complex. The selection of the format depends on the analyte size: competitive IA being applied for the detection of small analytes containing one binding site

for antibody recognition, while sandwich IA are applied to high molecular weight molecules that consist of two or more binding sites [17].

Since the labelling process reduces the activity of antibodies, high amounts of antibodies are needed, which is expensive, especially for sensitive detection antibodies. So, as an alternative, it can be useful to label secondary antibodies (anti-human, anti-rabbit, anti-mouse, etc.) that react with unlabelled primary antibodies (human, rabbit, mouse, etc.) at the solid support.

The most commonly IA format for laboratory routine analysis is the microtiter plate-based IA. This format uses a solid support for the antibody–antigen reaction and it requires the separation of the antibody-antigen complex from free antibodies.

3.3.2. Enzymatic methods

Enzymes are molecules, usually proteins that act as catalysts for a large number of biological processes. An enzymatic reaction begins with the formation of the enzyme-substrate complex, caused by the bounding of the substrate with the active site of the enzyme. Then the complex can return to its initial form or the product can be obtained.

$$E + S \leftrightarrows ES \leftrightarrows E + P$$

They have an important role in clinical analysis either as analytes or as reagents for their substrate determination. In this last case, they allow the direct analysis of biological samples without pretreatment, due to the specificity of enzymes for their substrates.

3.4. MICROFLUIDIC SYSTEMS

Lab-On-Chip (LOC) devices, which are a type of POCT systems based on microfluidics, have gained much attention due to their favourable characteristics in terms of reduced size and weight, very low sample and reagent consumption, reduced analysis time and, often, superior achievable performances in terms of limits of detection.

3.4.1. Microfluidic chip devices

Microfluidic technologies have a great potential for developing portable analytical devices due to the advantages in size, volume requirements and time for the analysis [18, 19, 20, 21, 22]. Traditional multiwell plates format commonly used in laboratory analysis are based on the

binding between the analytes in sample solution and the capture molecules immobilized on solid surfaces, while the analytes not bound to the capture molecules are removed during washing steps. These methods usually need relatively long incubation times and several hours are required to complete an analysis (from 1 to 24 h). Microfluidic immunosensors are able to overcome this limitation, since the increased surface-to-volume ratio makes it possible to have a more efficient transport in the immunoreactions, leading to a faster analysis. Indeed under flow in microchannels, this transport process is thought to be kinetically rapid due to the proximity of the analytes to the surface, [23] and the rapid replenishment of depleted analytes in the boundary layer by convective flow [24]. Moreover a miniaturized microchannel dimension provides the reduction of consumption of samples and reagents and automated integration with other functions, such as valves, pumps, mixers, and detectors allow achieving a POC goal [25]. For these reasons microfluidic systems have recently attracted great deal of attention as immunosensor platforms [26]. Microfluidic chips allow to develop arrays of specific capture probes on a functionalized surface, without impairing their binding ability. This system makes it also possible to perform multiplex analyses by spatially separating several reaction area, each of one specific for a different analyte that is recognized by its specific position.

Different methods can be employed to move liquids in microfluidics, such as pressure-driven flow, electro-osmosis, or acceleration. One of the simplest approaches for producing flow in microchannels is to use capillary forces [27]. Capillary-driven flow requires no peripheral equipment, and this concept is used for portable immunodiagnostic tests [28].

3.4.2. Paper-based analytical devices

An emerging microfluidic platform based on capillary forces, are those based on porous materials. Hydrophobic barriers patterned into a porous, hydrophilic material provide channels for the controlled and autonomous wicking of fluids to testing zones within a device. These materials operate independently of equipment and therefore make excellent substrates for the development of POCT diagnostic devices. Among porous materials, paper is an attractive substrate which allows producing diagnostic devices employing minimal infrastructure (e.g., a wax printer to pattern microfluidic channels and a pipette to dispense reagents) and inexpensive raw materials. In addition devices can be prototyped rapidly (ca. minutes from design to production) [29].

3.5. DEVELOPMENT OF PORTABLE ANALYTICAL DEVICES

3.5.1. Life-Marker detection in extraterrestrial environment

The search for life outside the Earth is one of the main goals of the scientific community. Nowadays, this research is focused on Mars as it presents some indications of possible past or present life: landforms produced by flowing water in the past [30] or the presence of methane in the Martian atmosphere [31] are some examples.

Current research strategies to find evidence of life in extra-terrestrial environment are based on the in-situ detection of organic molecules: amino acids, polycyclic aromatic hydrocarbons, nucleic acids, polysaccharides and other molecular systems characteristic of organized biological systems. Recently Life Marker Chip (LMC) [32] has been proposed to detect organics in the form of biomarkers that might be associated with extinct life, extant life or abiotic sources of organics.

LOC devices are extremely suitable for space missions and are under investigation in view of future planetary exploration. On this trail, the project Planetary Life Explorer with Integrated Analytical Detection and Embedded Sensors (PLEIADES), carried out at the Laboratory of Analytical and Bioanalytical Chemistry (headed by Prof. Aldo Roda) of the University of Bologna in collaboration with Sapienza University of Rome, aims to design and develop a portable biosensor for detecting life biomarkers.

An important step for the development of this system is the selection of a biomarker suitable for highlighting the presence of extinct or extant life. Although many chemistries could support life, the study of life in Mars is based on our knowledge of terrestrial life since, as on Earth, life is directly related with water. Adenosine triphosphate (ATP), was chosen as life biomarker. This molecule is composed by the nucleobase adenine, ribose and three phosphate groups and, according to a selection of molecular targets made for a European Space Agency's mission [33], it is classified as an extant biomarker. It is known for being an energy source and extracellular signalling mediator, thus, finding ATP on Mars would suggest the possibility of the presence of biological life.

In particular, PLEIADES project focuses on the development of a competitive IA based on CL detection for the identification of ATP. The IA will be implemented into a portable device (Figure 3.4) that is being developed exploiting a microfluidic network based on capillary forces

for the handling of samples and reagents, integrated with an array of thin film hydrogenated amorphous silicon (a-Si:H) photosensors for the detection of the analytical CL signal. The implementation of the CL bioassay into the compact and fully-integrated device will provide a new analytical platform for the multiparametric detection of bio-organic molecules outside of the Earth.

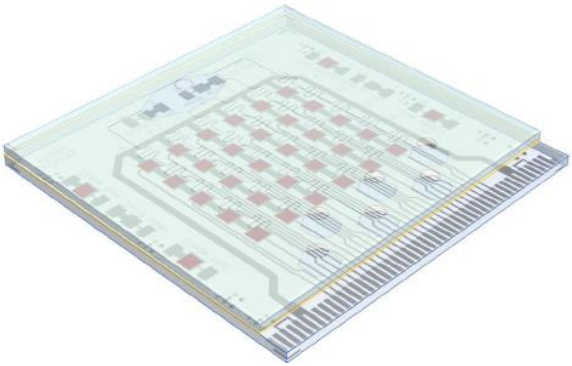

Figure 3.4 *Design of the microfluidic portable device expected to be developed in the PLEIADES project.*

3.5.2. Point-of-care testing for measurement of glycemia

Glucose is a chiral aldose monosaccharide that has two enantiomers: D-glucose, which is by far the most widespread in nature, and L-glucose. Due to its 6 carbon atoms, it is classified as a hexose and in aqueous solution it generally exists as a pyranose, which is its cyclic form resulting from the nucleophilic addition reaction between the aldehyde group at C-1 and the hydroxyl group at C-5. This cyclization provides a new stereogenic centre creating two diastereoisomers: α and β.

In the human body, there is an intrinsic system that monitors the concentration of glucose in blood. In a healthy body, glycemia is in the range of 70 and 110 mg/dL (3,9 and 6,1 mM). Higher (hyperglycemia) or lower (hypoglycemia) values may derive from different pathologies. Diabetes is a common example of hyperglycemia.

There are several LOC enzymatic devices that make life easier for diabetes patients. They are all based on the glucose oxidation to gluconolactone, described in Figure 3.5, catalysed by the glucose oxidase (GOx) enzyme. GOx is a dimeric protein that acts specifically on β-D-glucose (not on α-D-glucose).

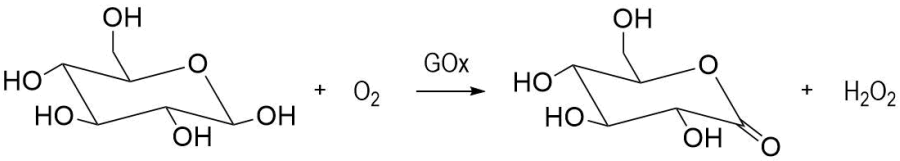

Figure 3.5 *Oxidation of β-D-glucose catalysed by the enzyme glucose oxidase, producing gluconolactone and hydrogen peroxide.*

In the first devices, the oxygen of the solution consumed during the reaction was determined amperometrically. However, to avoid the intrinsic limit due to the dependence of the signal on the initial oxygen concentration, amperometric biosensors of second generation had been developed. In that case, after the glucose oxidation, the enzyme is oxidized by a redox mediator (e.g. hexacyanoferrate (III) ion) and it is then oxidized at the working electrode producing a measurable electric current, whose intensity under standardized conditions is proportional to the concentration of glucose.

As an alternative, new emerging paper-based device platform can be used for developing portable analytical devices that are easy-to-use, cheap and fast. In particular, in order to obtain a sensitive and accurate analysis, it is possible to exploit a CL enzymatic reaction in which glucose is oxidised by GOx producing hydrogen peroxide. The hydrogen peroxide generated by this reaction, in presence of luminol and hexacyanoferrate (III), allows the production of photons which can be detected using portable instrumentation like CMOS device.

4. OBJECTIVES

The present work is focused on the study of two different chemiluminescent bioanalytical assays.

On one hand, a chemiluminescent immunoassay for detection of ATP is optimised. The aim of that study is three-fold:

1. To choose the most suitable reagents and type of immunoassay in order to find the better conditions for the chemiluminescent competitive immunoassay.
2. To optimise chemical conditions of the competitive immunoassay selected for obtaining suitable analytical performances.
3. To make a calibration curve.

On the other hand, the aims of the study about paper-based device with chemiluminescent detection for glucose quantification in serum samples are:

1. To adapt a device tested before using a CCD camera to the use of a more compact and portable CMOS sensor for the detection.
2. To make a calibration curve in the range of 50-250 µM of glucose in buffer solution of carbonate 0,1 M and another in human serum diluted 1:50 (V/V) to evaluate the matrix effect.
3. To compare the calibration curves in carbonate 0,1 M buffer solution obtained using CMOS with those obtained in a previous study using CCD.

5. EXPERIMENTAL SECTION

5.1. DEVELOPMENT OF CHEMILUMINESCENT IMMUNOASSAY FOR DETECTION OF ATP

5.1.1. Reagents

Non-fat dried milk bovine (Sigma Aldrich Chemical)

Streptavidin (Thermo Fisher Scientific, 10 mg/mL)

Bovine Serum Albumin (BSA) (Sigma Aldrich Chemical)

Boric acid (Carlo Erba Reagents)

Sodium carbonate (Carlo Erba Reagents)

Sodium chloride (Carlo Erba Reagents)

Sodium dihydrogen phosphate monohydrate (Carlo Erba Reagents)

Disodium phosphate anhydrous (Carlo Erba Reagents)

Phosphate Buffered Saline (PBS)

Adenosine triphosphate (ATP) (Sigma Aldrich Chemical)

HRP conjugated to biotin (HRP-Biotin) (Invitrogen)

ATP conjugated to biotin (ATP-Biotin) (Enzo Life Sciences)

ATP conjugated to Ovalbumin (ATP-OVA) (Cloud-Clone Corp, 0,1 mg/mL)

ATP conjugated to BSA (ATP-BSA) (Cloud-Clone Corp, 0,1 mg/mL)

Antibody Anti-ATP in rabbit (Abcam)

Antibody Anti-ATP in rabbit (Cloud-Clone Corp)

Antibody AntiRabbit conjugated to HRP (AntiRabbit-HRP) (Sigma Aldrich Chemical)

Antibody Anti-Ovalbumin in mouse (Sigma Aldrich Chemical)

Antibody Anti-Ovalbumin in rabbit (Sigma Aldrich Chemical)

Antibody AntiMouse conjugated to HRP (AntiMouse-HRP) (Sigma Aldrich Chemical)

Chemiluminescent substrate for HRP (Supersignal ELISA Femto) (Thermo Fisher Scientific)

5.1.2. Instruments

Analytical balance (Sartorius)

pH Meter (Beckman Coulter)

Nitrocellulose (GE Whatman)

96-well microplate (Thermo Fisher Scientific)

Camera (MagZero 2 PRO, MagZero, Pordenone) based on CCD sensor (Sony ICX285 (1360 x 1024 pixel))

Luminoskan Ascent Microplate Luminometer (Thermo Fisher Scientific)

5.1.3. Selection of the reagents and optimization of the experimental conditions: nitrocellulose-based chemiluminescent immunoassay

Optimization of the experimental conditions of the immunoreactions were performed by preliminary measurements using nitrocellulose membranes as platform allowing an easy and reproducible analysis. Competitive IA was selected as the most suitable format since ATP is a small molecule which is not indicated for a non-competitive ("sandwich") method. Different reagents and different type of IA were tested to find the better conditions for the CL competitive IA. Being a competitive IA, these preliminary tests were performed in absence of ATP in the samples in order to select the reagents able to achieve the maximum signal (signal decreases at the increase of analyte concentrations) and to evaluate the performance of the immunoreagents. Three different type of IA were investigated:

1. Indirect competitive immunoassay (a):

This approach, shown in Figure 5.1, is based on the competition between ATP-Biotin and ATP present in the sample for binding the Anti-ATP antibody. Detection is performed by adding an anti-species antibody conjugated to HRP. This procedure required the preliminary immobilization of streptavidin on nitrocellulose membrane. Streptavidin has the task of binding ATP-Biotin which is too small molecule for being immobilized directly on nitrocellulose or plastic support. In this format two different antibodies were tested: one from Abcam and the other from Cloud-Clone Corp.

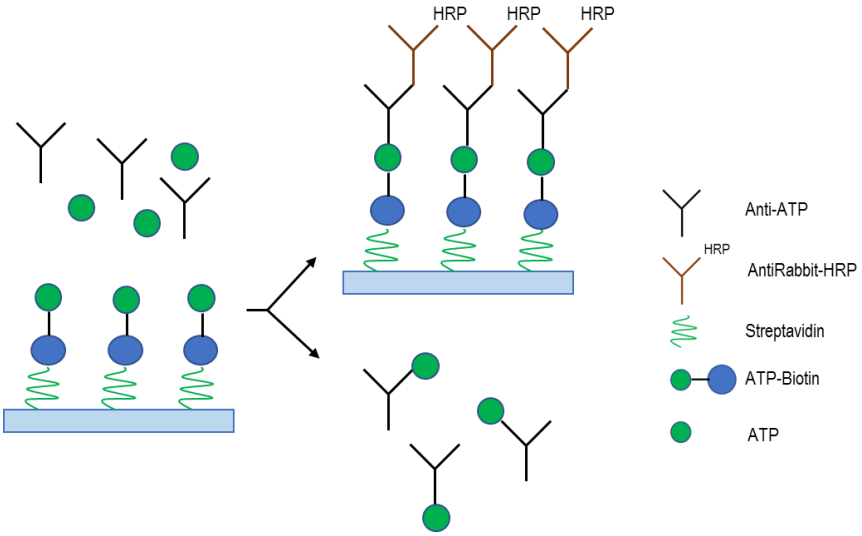

Figure 5.1 *Indirect competitive immunoassay (a).*

Streptavidin was immobilized on nitrocellulose membrane at the previously chosen concentration in borate buffer 0.05 M at pH 5. The immobilization was performed by spotting 1 μL of different solutions on nitrocellulose membrane. After the spot was dried, membranes were saturated by incubating them for 1 h in a solution of non-fat-dried milk 5% (V/V) diluted in PBS. Membranes were then washed three times using PBS (washing step). Then membranes were incubated for 1 h in a solution containing ATP-Biotin diluted 1:1000 in PBS (V/V). After washing step, membranes were treated for 1 h with a solution containing Anti-ATP antibody produced in rabbit diluted 1:500 in PBS (V/V). After another washing step membranes were incubated with AntiRabbit-HRP diluted 1:1000 in PBS (V/V) for 1 h. Finally, strip were washed once again and then CL signals were acquired by adding CL substrate and using CCD camera with integration time of 5 s.

2. Indirect competitive immunoassay (b):

This approach, shown in Figure 5.2, consists on the immobilization of ATP-OVA or ATP-BSA on nitrocellulose membrane. ATP present in the sample and immobilized ATP-OVA or ATP-BSA compete for binding Anti-ATP antibody. Detection is performed by adding an anti-species antibody conjugated to HRP.

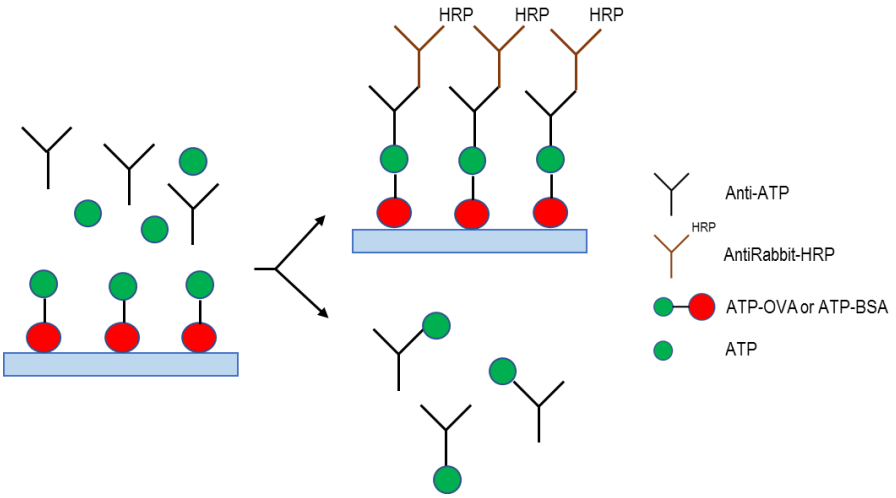

Figure 5.2 *Indirect competitive immunoassay (b).*

The procedure was performed using two different antibodies Anti-ATP (one purchased from Abcam and the other from Cloud-Clone Corp) in order to choose the one that gives suitable analytical performance. ATP-OVA was immobilized on nitrocellulose membrane at different dilutions (1:10, 1:100, 1:1000 (V/V)) in PBS buffer. The immobilization was performed by spotting 1 μL of different solutions on nitrocellulose membrane. After the spot was dried, membranes were saturated by incubating them for 1 h in a solution of non-fat-dried milk 5% (V/V) diluted in PBS. Membranes were subjected to a washing step. Then membranes were incubated for 1 h in a solution containing Anti-ATP produced in rabbit at different dilutions (1:1000, 1:10000, 1:100000 (V/V)) in PBS. After washing step membranes were incubated for 1 h with AntiRabbit-HRP diluted 1:1000 (V/V) in PBS. Finally, strip were washed once again and then CL signals were acquired by adding CL substrate and using CCD camera with integration time of 5 s.

The Anti-ATP antibody selected was used to do the same procedure immobilizing ATP-BSA.

3. Direct competitive immunoassay:

This approach, shown in Figure 5.3, consists on the immobilization of Anti-ATP produced in rabbit on nitrocellulose membrane. The ATP present in the sample and ATP-OVA compete for

binding the immobilized antibody. Detection is performed by adding in sequence Anti-Ovalbumin produced in mouse and AntiMouse-HRP.

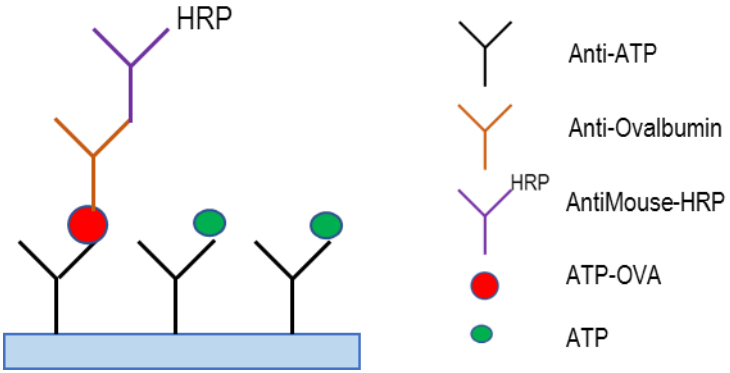

Figure 5.3 *Direct competitive immunoassay.*

Antibody Anti-ATP (purchased from Abcam) was immobilized on nitrocellulose membrane at different dilutions (1:100, 1:1000, 1:10000 (V/V)) in PBS. The immobilization was performed by spotting 1 µL of different solutions on nitrocellulose membrane. After the spot was dried, membranes were saturated by incubating them for 1 h in a solution of non-fat-dried milk 5% (V/V) diluted in PBS. Membranes were subjected to a washing step. Then membranes were incubated for 1 h in a solution containing ATP-OVA diluted 1:500 (V/V) in PBS. After washing step membranes were incubated with Anti-Ovalbumin antibody produced in mouse diluted 1:500 (V/V) in PBS. Then membranes were washed and incubated for 1 h with AntiMouse-HRP diluted 1:1000 (V/V) in PBS. Finally, strip were washed once again and then CL signals were acquired by adding CL substrate and using CCD camera with integration time of 5 s.

For each experiment, a control strip was made to check if the immobilization had been correctly done. After the immobilization and saturation step, the control membrane was treated as follow:

1. Immobilization of streptavidin: the membrane was treated for 1 h with HRP-Biotin diluted 1:500 (V/V) in PBS. After washing step, CL signals were acquired by adding CL substrate and using CCD camera with integration time of 5 s.

2. Immobilization of Ovalbumin-ATP: the membrane was treated for 1 h with Anti-Ovalbumin in rabbit diluted 1:500 (V/V) in PBS. Then membranes were washed and incubated for 1 h with AntiRabbit-HRP diluted 1:1000 (V/V) in PBS. After washing step, CL signals were acquired by adding CL substrate and using CCD camera with integration time of 5 s.
3. Immobilization of Anti-ATP produced in rabbit: the membrane was treated for 1 h with AntiRabbit conjugated to HRP diluted 1:1000 (V/V) in PBS. After washing step, CL signals were acquired by adding CL substrate and using CCD camera with integration time of 5 s.

5.1.4. Experimental procedure of CL-based indirect competitive immunoassay in microplate format

An assay was made to ensure the immobilization of ATP-OVA and the formation of the competitive IA selected on the microplate format. Thus, as in nitrocellulose assays, this first assay was made without the target analyte.

A solution of ATP-OVA 10^{-4} mg/mL in carbonate buffer (pH 10, 0.05M) was used for coating 96-well microplate with 100 µL per well and incubated overnight at 4°C. Wells were washed three times using for each well 300 µL of PBS (pH 8, 0.2 M) containing 3% BSA (w/V). The wells were saturated with the same solute ion for 4 h at 4°C. In order to verify the correct immobilization of ATP-OVA, wells were incubated for 1 h at room temperature with different dilutions of Anti-ATP (1:100, 1:1000, 1:10000 (V/V)) in PBS (100 µL per well). Control wells were incubated with Anti-Ovalbumin at the same dilutions and conditions. Once performed a washing step, wells were treated for 1 h at room temperature with AntiRabbit-HRP diluted 1:2000 (V/V) in PBS (100 µL per well). Finally, after a washing step, 100 µL of CL substrate was added and the CL signals were acquired using a luminograph with integration time of 200 ms.

Once the immobilization was confirmed, parameters as incubation time and the concentration of the Anti-ATP antibody were studied to define the procedure to make a calibration curve of the analyte. For that assays, solutions of ATP at different concentrations were used.

5.1.5. Data elaboration

To obtain quantitative information, the mean photon emission intensity was measured and subtracted from background signal. Background signal was recorded using a well in which, after immobilization of ATP-OVA and saturation steps, was performed only the last step with incubation of AntiRabbit-HRP. Then to generate the calibration curve, it was calculated the ratio B/B_0 in which B is the signal obtained for each analyte concentration while B_0 is the maximum signal obtained in the absence of target analyte.

As in every competitive method, the B_0 value corresponds to the maximum binding of the tracer to the solid phase, while B is the signal for a specific concentration of the analyte where only a fraction of the tracer is bound to the solid phase. Therefore, the B/B_0 ratio represent the fraction of the tracer that has been displaced by a specific concentration of the analyte and is included between 0 and 1. Values of B/B_0 were then plotted against the log of analyte concentration obtaining a sigmoidal curve that is described by a four-parameter logistic function.

5.2. PAPER-BASED DEVICE WITH CHEMILUMINESCENT DETECTION USING CMOS FOR THE DETERMINATION OF GLUCOSE

5.2.1. Reagents

Glucose oxidase from *Aspergillus niger* (Sigma Aldrich Chemical, 210 U/mg)

Glucose (Sigma Aldrich Chemical)

Hexacyanoferrate (III) of potassium (Sigma Aldrich Chemical)

Luminol (5-Amino-2,3-dihydrophthalazine-1,4-dione, as a sodium salt) (Sigma Aldrich Chemical)

Hydrogen peroxide (VWR Chemicals, 30%)

Sodium carbonate (Carlo Erba Reagents)

Phosphate Buffered Saline (PBS)

Human serum

5.2.2. Instruments

Analytical balance (Sartorius)

pH Meter (Beckman Coulter)

Heating plate Arex (Velp Scientifica)

Replicator 2X Experimental 3D Printer (MakerBot)

Chromatographic paper (Whatman CHR, 20 x 20 cm) (Sigma Aldrich)

Camera (MagZero 2 PRO, MagZero) based on CCD sensor (Sony ICX285 (1360 x 1024 pixel))

CMOS sensor (Micron® Imaging MT9M001, Micron Technologies)

5.2.3. From CCD to CMOS

The analytical device was developed at first to be used in combination with a CCD camera. In this configuration, the darkroom was connected to the emission detection system which consisted of a camera based on a commercially available CCD sensor. The camera was equipped with a dual-cell Peltier thermoelectric cooling system that allowed to reduce sensor temperature to 40 ° C below room temperature. The possibility for the CCD sensor to operate at low temperatures is fundamental for reducing thermal background noise and for achieving the detection even of weak CL signals. Moreover the camera was used in ”contact imaging” configuration: the paper support was placed directly in contact with the CCD sensor through a fiber optic faceplate. The faceplate directly transfer CL signals to the CCD sensor allowing to obtain a more compact device and to increase the sensitivity by increasing the efficiency of collected light. The fiber optic element also acted as a thermal insulation, allowing the CCD sensor to cool down without affecting the temperature of the analytical module in which the CL reactions occur.

Using this detector, the experimental parameters were optimized and the assay showed good analytical performances. However, although the device was compact and portable, reduction of power consumption, greater compactness and low-cost are required to obtain a LOC system.

In this study, this assay was implemented in a fully-integrated system using a monochromatic CMOS sensor for the detection of CL signals (pixel size: 5.2µm x 5.2µm). CMOS sensor have a 1/2-inch CMOS active-pixel digital image sensor. It incorporates sophisticated camera functions and it is programmable through a simple two-wire serial interface. This megapixel CMOS image sensor is characterized by low-noise CMOS imaging

technology that achieves CCD image quality (based on signal-to-noise ratio and low-light sensitivity) while maintaining the inherent size, cost, low power consumption and integration advantages of CMOS.

5.2.4. Origami device

Origami, the art and science of paper, is a folding technique in which 3D objects are built from a planar paper. Recently this technique has been exploited to develop 3D paper-based microfluidic devices.

The design of the origami paper-based device used in this study, shown in Figure 5.4, was made by using PowerPoint. Through the 3D printer and solid wax ink, the design was printed on chromatographic paper. Then, the printed paper was heated for a few minutes at approximately 120 °C in a heating plate. With warming, the wax melts and penetrates into the paper pores generating the hydrophobic areas, which delimit the circular hydrophilic areas (active areas of the device that will contain the reagents) and the separation lines that make the device bendable (they become more flexible than the printed areas).

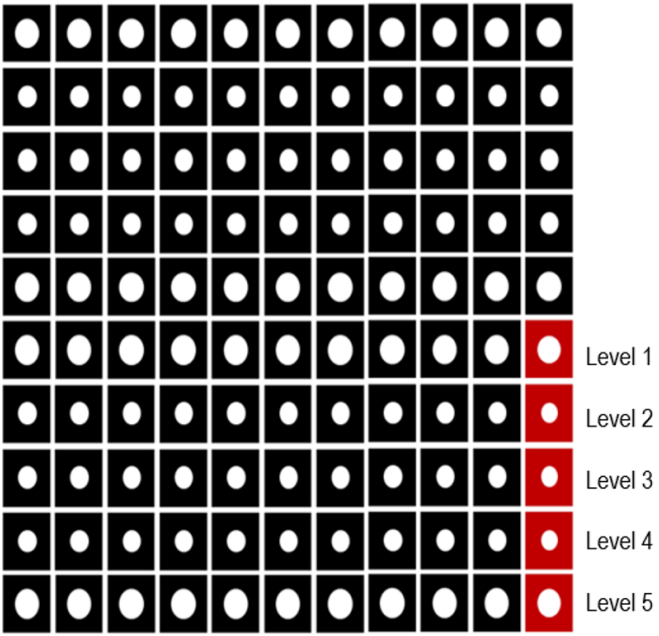

Figure 5.4 *Design of the hydrophobic areas of the origami device. In red, a single device.*

In order to finish the preparation, the devices were cut individually and the reagents were added in every single device. After the addition of reagents in the proper circular area, the devices were left to dry protected from light. The function and the reagents contained in the various hydrophilic areas are described in Table 5.1, while Figure 5.5 shows the development of the device.

Level	Function and reagents
1 – Hydrophilic area, Ø = 8 mm^2	Allows the uniform distribution of the buffer solution injected used as eluent. The bigger area guarantees a more homogeneous migration of the eluent on that level.
2 – Hydrophilic area, Ø = 6 mm^2	Contains 5 µL of GOx 1 U in buffer solution of PBS 0,01 M (pH = 7,5). It is also the level where 10 µL of the sample, diluted 1:50 (V/V), containing glucose will be added.
3 – Hydrophilic area, Ø = 6 mm^2	Avoid the contact between the levels 2 and 4 when the device is folded
4 – Hydrophilic area, Ø = 6 mm^2	Contains 10 µL of hexacyanoferrate (III) of potassium 0,02 M in buffer solution of carbonate 0,1 M (pH = 10,0)
5 – Hydrophilic area, Ø = 8 mm^2	Contains 10 µL of luminol 0,2 M in buffer solution of carbonate 0,1 M (pH = 10,0). The bigger area allows this level to absorb a higher volume of eluent than the others favouring the elution of the reagents to that level
6 – Transparent sticky tape	Protect the camera from the eluent that has gone through all the levels

Table 5.1 *Function and reagents content in each hydrophilic area of the origami's device.*

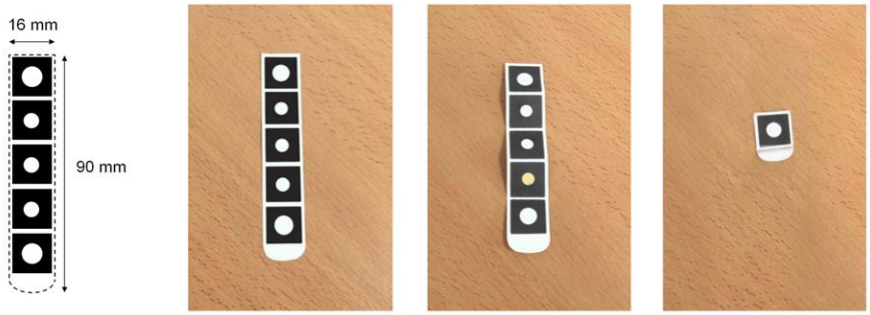

Figure 5.5 *Steps on origami's device development from left to right: computer design, printed device, device after the thermic treatment and the addition of the reagents, and folded final configuration.*

5.2.5. Adapters for origami-detection

An important tool that ensures keeping the device in folded position during the measurement and that provides a slight pressure to get close contact between the various levels of the device is the holder (Figure 5.6). The holder presents three openings: the origami device can be inserted through its side opening, whereas the upper and lower allow the insertion of the eluent to the first level and the measurement of the CL signal from the last one, respectively.

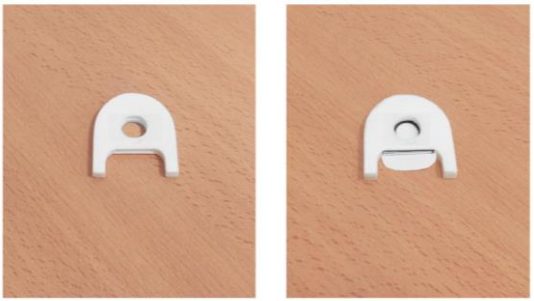

Figure 5.6 *Holder with and without the origami device inside.*

The connection between the holder and the CMOS camera is made by a dark chamber. This chamber does not allow the entrance of light into the system allowing the CL measure, guarantees the reproducible positioning of the holder over the faceplate of the CMOS and it also incorporates a hole through which a syringe can introduce the eluent in the first level of the

origami device. Origami device was placed at a distance of 2.5 cm from CMOS sensor in order to focus the CL emission area. The whole instrumentation is shown in Figure 5.7.

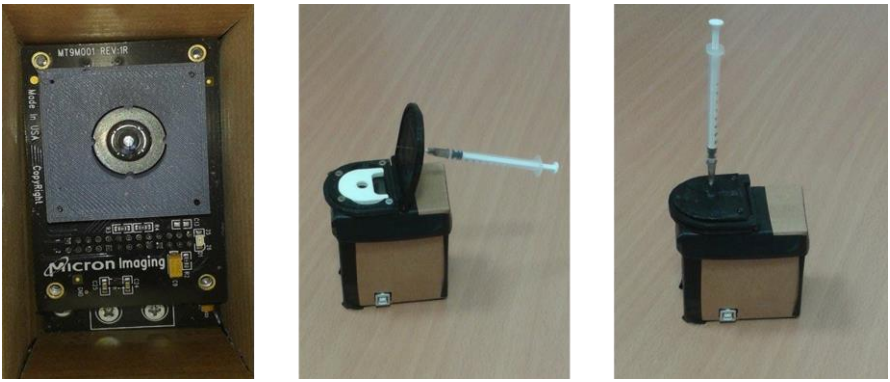

Figure 5.7 *From left to right: CMOS camera in the device structure, opened device with the holder inside and device ready for the assay.*

Both instruments were made of acrylonitrile-butadiene-styrene copolymer by using a commercial 3D printer.

5.2.6. Experimental procedure

The assay starts with the addition of 10 µL of the sample to the level 2 of the device. After 10 minutes (which is the time required for the enzymatic reaction between glucose and the enzyme GOx for producing hydrogen peroxide) CL measurement is performed.

For the measurement, the folded origami device is introduced in the holder and into the dark chamber as explained in paragraph 5.2.5. When 100 µL of the eluent are added by using the syringe, the hydrogen peroxide produced in level 2 and the solution of hexacyanoferrate (III) of potassium present in level 4 move to level 5 where the presence of luminol allows the CL reaction.

A preliminary test was performed in order to compare the signal-to-noise ratio obtained using a CCD and a CMOS camera, respectively, and to ensure the reliability of the results obtained using the CMOS camera. Thus, instead of GOx and glucose, 10 µL of 100 µM hydrogen peroxide were added to the level 2 of the device.

On the other hand, calibration curves were generated using glucose standard solutions in the range between 50 µM and 250 µM. Calibration curve was constructed by adding known amounts of glucose standard solutions to human serum diluted 1:50 (V/V). This was compared

with a calibration curve obtained in carbonate buffer solution 0,1 M (pH = 10,0) to evaluate the matrix effect.

5.2.7. Data elaboration

The CL signal produced when the elution buffer on level 1 migrates through the underlying layers has a transient character (starts when the reagents come into contact and then declines slowly due to substrate consumption).

It is known that for flash kinetic CL signals the total emission measurement results in better quantitative results than the evaluation of its maximum intensity. In principle, total emission could be measured by acquiring a single image with a sufficiently long exposure time but in practice it is not possible because the high number of photons collected would lead to saturation of the CMOS sensor with signal loss. This eventuality is avoided by acquiring a sequence of images with relatively short exposure times.

Hence, sequence of images were acquired with a time exposure of 1 second and were analysed by using an ImageJ software v.1.46 (National Institute of Health, Bethesda, MD). This software allows the quantification of the CL signal of each image, thus, it was possible to represent the variation of the CL signal over the time. The mean photon emission intensity was measured in the areas corresponding to the area of interest. Each was subtracted from the mean background signal measured in the adjacent areas. The obtained values were integrated in order to obtain the total CL intensity emission. Calibration curves were obtained by plotting CL intensity values corresponding to different concentration of glucose against the glucose concentration and fitting the experimental data with a linear two-parameter logistic function.

6. DEVELOPMENT OF CHEMILUMINESCENT IMMUNOASSAY FOR DETECTION OF ATP: DISCUSSION

6.1. OPTIMIZATION OF THE METHOD ON NITROCELLULOSE PLATFORM

The results obtained for the three different competitive type of IA tested on nitrocellulose support in absence of the target analyte are described in the next paragraphs.

6.1.1. Indirect competitive immunoassay (a)

First, conditions for immobilizing streptavidin were evaluated. Thus, control strips were prepared by immobilizing different concentrations of streptavidin (from 10 mg/mL to 0,1 mg/mL) and dilutions were performed in borate buffer 0.05 M at pH 5. After making the complete procedure for the control strip described on the experimental part, the results obtained were those shown in Figure 6.1. The CL signal was obtained only at concentrations 10 and 1 mg/mL. The concentration of 10 mg/mL was chosen as the most appropriate from which to work.

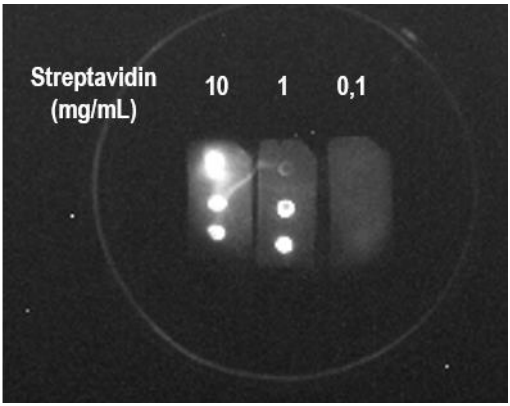

Figure 6.1 *CL images of different concentrations of streptavidin spotted on nitrocellulose.*

Once selected the concentration of streptavidin of 10 mg/mL, it was tested the immunological method, by treating a nitrocellulose membrane as described in paragraph 5.1.3. Independently of the Anti-ATP antibody used, the tested method gave no results, which means

that competitive IA structure was not formed. In contrast, control membrane present a sharp and intense CL signal, confirming the correct immobilization of streptavidin.

6.1.2. Indirect competitive immunoassay (b)

The second indirect competitive IA was tested. First, in order to select the most adequate Anti-ATP antibody and after the use of each one in this format, the CL signal obtained was compared. As shown in Figure 6.2, while membrane treated with Anti-ATP from Abcam did not show any CL signal, the membrane treated with Anti-ATP from Cloud-Clone Corp. showed an intense CL signal in correspondence of the spot of ATP-OVA. Hence, Anti-ATP from Cloud-Clone Corp was selected as the most suitable antibody to the test.

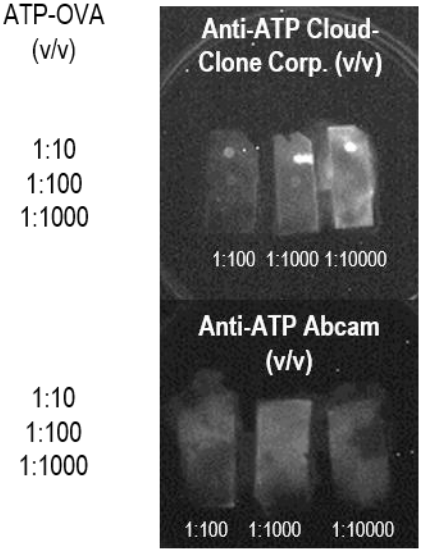

Figure 6.2 *CL images of the membranes treated with two different antibodies.*

Together with ATP-OVA, also ATP-BSA was immobilized and tested in the same conditions in order to select the best option for the performance of the assay. The Cloud-Clone Corp Anti-ATP was used in this assay. Comparing the two options, showed in Figure 6.3, ATP-OVA was chosen since it allows to obtain better performance and higher CL signals.

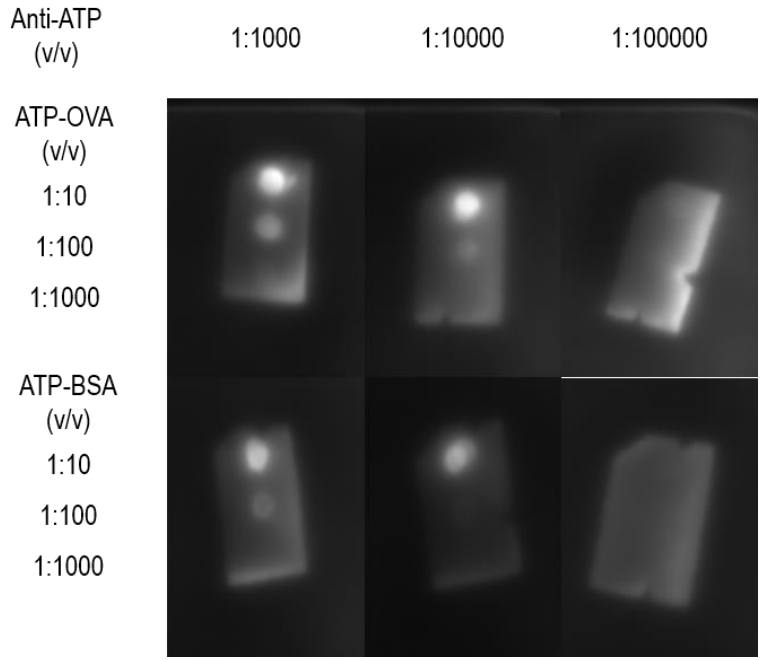

Figure 6.3 *CL signals obtained after applying the complete protocol to different concentrations of ATP-OVA and ATP-BSA, respectively, using different concentrations of antibody.*

In each assay, also the control strip was performed, obtaining CL signal and demonstrating that ATP-OVA and ATP-BSA were correctly immobilized.

6.1.3. Direct competitive immunoassay

As shown in Figure 6.4, Anti-ATP was correctly immobilized as evidenced by CL image of the control membrane where the spot corresponding to the maximum immobilized concentration of Anti-ATP showed a strong CL signal. On the contrary the membrane subjected to the complete protocol showed no CL signals.

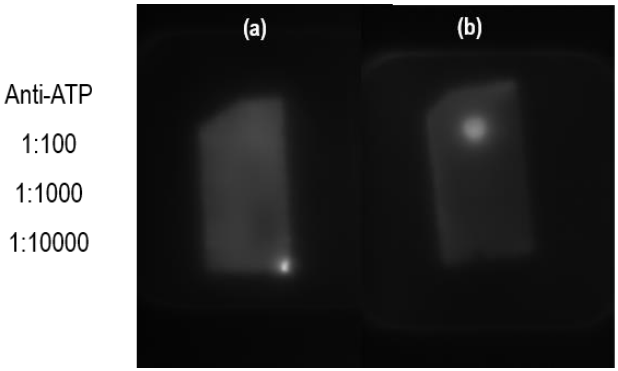

Figure 6.4 *(a) CL images of the membrane subjected to the complete protocol; (b) control membrane.*

6.2. OPTIMIZATION OF CHEMILUMINESCENT IMMUNOASSAY ON MICROPLATE FORMAT

Accordingly to the obtained results, the indirect competitive immunoassay (b) was the selected approach. The Anti-ATP antibody chosen for the immunoassay was the one from Cloud-Clone Corp. The protocol was transferred to 96-microwell plate format.

6.2.1. Immobilization of ATP-OVA

The immobilization of ATP-OVA was studied as described in paragraph 5.1.4. Figure 6.5 shows the results obtained for the competitive immunoassay applied. CL signals are proportional to antibodies concentrations, confirming the correct immobilization of ATP-OVA and the formation of the competitive IA structure.

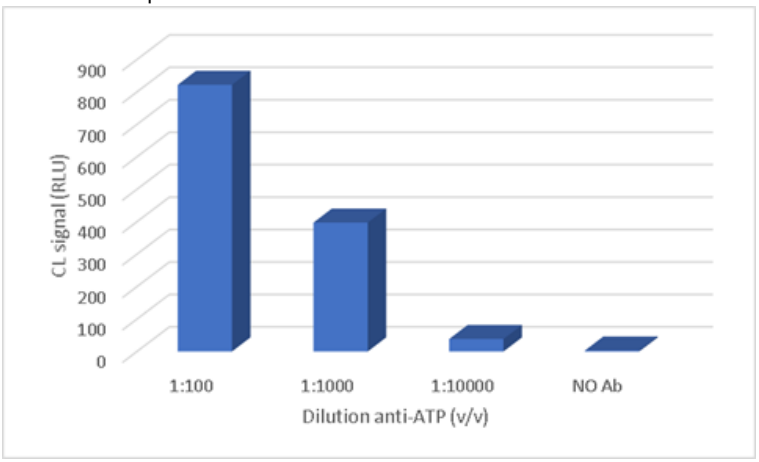

Figure 6.5 *CL signal variation respect to Anti-ATP dilutions.*

6.2.2. Incubation time

In order to select the proper incubation time for the competitive step of the IA, two different approaches were tested. Following procedures were tested:

a) Solutions of 100 µL containing different amount of ATP (from 20 to 0,3 nmol) and Anti-ATP diluted 1:1000 (V/V) in PBS were added into wells, where ATP-OVA had been previously immobilized and incubated for 1 h.

b) Solutions of 100 µL containing different amount of ATP (from 20 to 0,3 nmol) and Anti-ATP diluted 1:1000 (V/V) in PBS incubated for 1 h out of wells. Then these solutions were transferred into wells, where ATP-OVA had been previously immobilized, and incubated for 1 h.

The last incubation, common for both procedures, was made in a dilution of AntiRabbit-HRP 1:1000 (V/V).

As showed by Figure 6.6 while option (a) did not allow to discriminate between different concentrations of ATP, the option (b) allowed to obtain slightly changes of CL signals as the concentrations change. Probably this difference is due to the fact that Anti-ATP antibody has a higher compatibility with the ATP-OVA respect to ATP molecule, so a preliminary incubation of ATP with Anti-ATP is required.

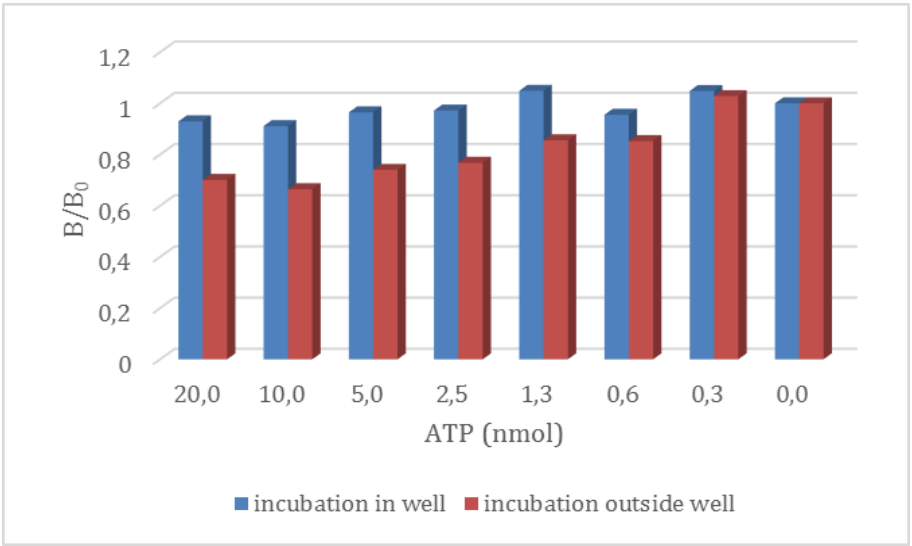

Figure 6.6 *Variation of CL signal with ATP amount changes respect to maximum signal at 0 nmol of ATP (maximum signal) using different protocol for incubation.*

Then it was also tested a lower incubation time (30 min) of the pre-mixed solution into wells. In this case, as shown in Figure 6.7, the CL signals were lowered significantly compromising the sensibility of the assay.

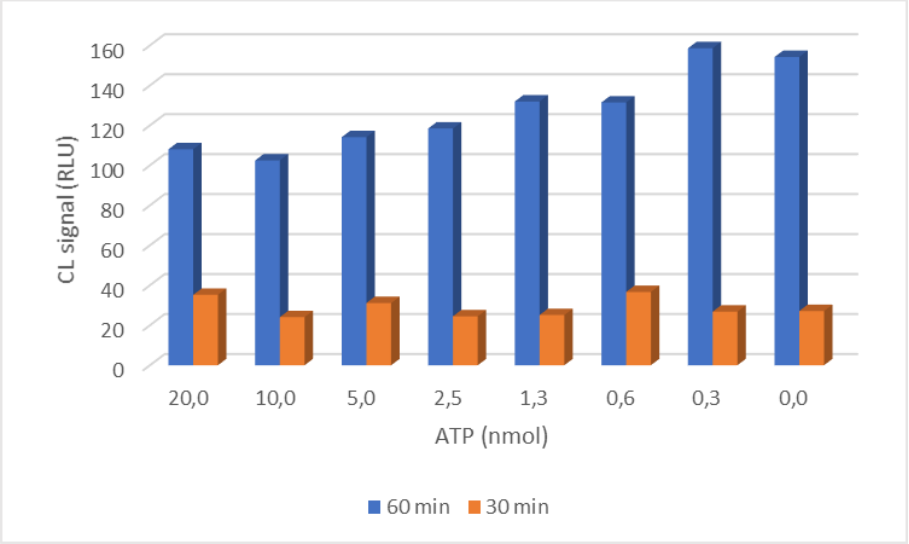

Figure 6.7 *Variation of CL signal with ATP amount changes using different time of incubation out wells.*

6.2.3. Dilution of Anti-ATP antibody

An important parameter that has to be evaluated is the dilution of Anti-ATP antibody. In order to select the proper dilution, tests were performed using different amount of ATP (0, 2, 20, 200 nmol) in presence of different dilution of Anti-ATP (1:1000, 1:5000, 1:10000 (V/V) in PBS). ATP-OVA 10^{-4} mg/mL had been previously immobilised and the last incubation was made in an AntiRabbit dilution 1:1000 (V/V).

Results are showed in Figure 6.8. The dilution that allowed to significantly distinguish between different concentrations of ATP is 1:5000. In fact, dilution 1:1000 allowed to discriminate the blank samples from other concentration but it was not possible to distinguish different concentration of ATP from each other. Dilution 1:10000 showed a significant change in CL signal between 2 and 20 nmol of ATP but there was no difference between 20 and 200 nmol.

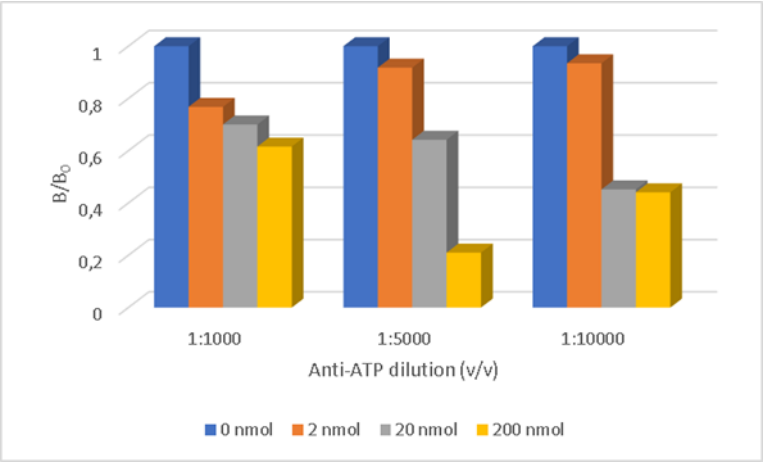

Figure 6.8 *Selection of the proper dilution of Anti-ATP.*

6.3. CALIBRATION CURVE

In the following lines, the procedure used to make the calibration curve of ATP is described. It is based on the results obtained in the previous section.

A solution of ATP-OVA 10^{-4} mg/mL in carbonate buffer (pH 10, 0.05M) was used for coating 96-well microplate with 100 µL per well and incubated overnight at 4°C. Wells were washed three times using for each well 300 µL of PBS (pH 8, 0.2 M) containing 3% BSA (w/V). The wells were saturated with the same solute ion for 4 h at 4°C. In the meanwhile, ATP standard solutions with different quantity of ATP (in the range of 0,0025 – 250 nmol) and Anti-ATP antibody produced in rabbit diluted 1:5000 in PBS (V/V), incubated for 1 h at room temperature. After washing microplates well as previously described, 100 µL of each solution of ATP and anti-ATP antibody produced in rabbit was transferred into wells and incubated for 1 h at room temperature. A washing step was performed and a solution containing Anti-Rabbit-HRP diluted 1:1000 (V/V) in PBS was added into wells (100 µL per well) and incubated 1 h at room temperature. Finally, after a washing step, 100 µL of CL substrate was added and the CL signals were acquired using a luminograph with integration time of 200 ms.

Calibration curve obtained is shown in Figure 6.9. Being a competitive type format, the decrease of the B/B_0 ratio was directly proportional to the amount of the analyte in the sample. The results of repeated calibration curves demonstrated a good reproducibility with an average

of the relative standard deviation associated with each point of the calibration curve of about 10%. The limit of detection (LOD) was estimated as the number of moles corresponding to the blank value minus three times its standard deviation. The obtained value was 0,01 nmol and the dynamic range extend from 0,01 to 80 nmol. Results were expressed in nmol and not in concentration, as the nature of the sample is still unknown.

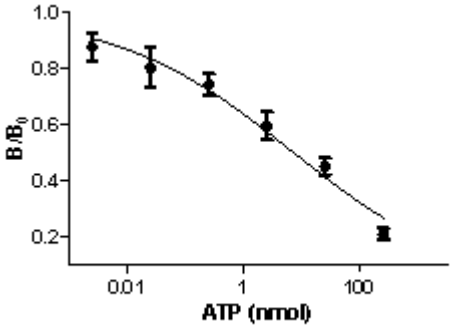

Figure 6.9 *Calibration curve.*

7. PAPER-BASED DEVICE WITH CHEMILUMINESCENT DETECTION USING CMOS FOR THE DETERMINATION OF GLUCOSE: DISCUSSION

7.1. CMOS SENSOR DETECTABILITY AND RESOLUTION

Preliminary test was performed as described in section 5.2.6. A solution of hydrogen peroxide 100 μM was used in order to compare the signal-to-noise ratio obtained with the reference CCD camera and CMOS sensor. As reported in Figure 7.1, CCD showed a higher signal-to-noise ratio compared with that obtained using a CMOS sensor. This is due to the fact that CMOS detector is less sensitive than a CCD because the latter is cooled at 40 °C below room temperature and presents larger pixel size. The CL intensity profiles measured across the circle show that the peaks are resolved at the baseline, showing that resolution offered by the different detector was comparable.

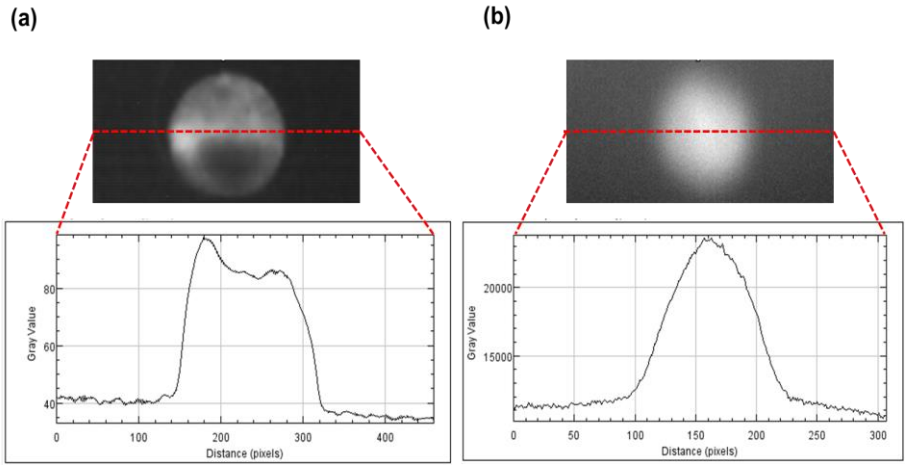

Figure 7.1 *Comparison of the signal-to-noise ratio of the CL signal, obtained in the middle of the kinetic profile using, using (a) CMOS sensor and (b) CCD camera.*

7.2. CALIBRATION CURVE

Calibration curve was generated adding glucose standard solutions in the range of 50 to 250 µM in carbonate buffer solution. Figure 7.2 shows the kinetic profile of the CL signal obtained. The kinetics are coherent as the CL signal area is proportional to the concentration of glucose.

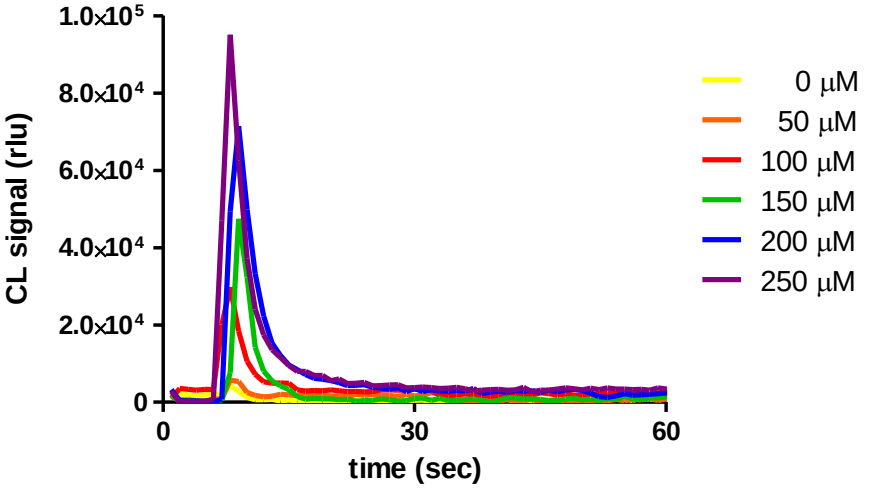

Figure 7.2 *Kinetic profile of CL signal obtained for the range of 50 – 250 µM of glucose.*

Comparison between calibration curve obtained with CCD and with CMOS is reported in Figure 7.3. The calibration curve performed using CMOS, y = (2160 ± 80)x + (-18000 ± 12000), presented a better linear correlation, $R^2 > 0,99$, than the one obtained using CCD, y = (7,0 x 10^7 ± 3 x 10^6)x + (2 x 10^8 ± 4 x 10^8), that has a linear correlation of $R^2 > 0,97$. This is probably due to the fact that CMOS' curve has one fewer point on it.

The limit of detection (LOD) was estimated as the concentration corresponding to the blank value plus three times its standard deviation. The obtained value was then interpolated in the calibration curve. The obtained values were 30 µM using CMOS and 10 µM using a CCD while the dynamic ranges of the method extended from 30 to 250 µM and from 10 to 250 µM, respectively. Even if CCD camera allowed to obtain a lower LOD, nevertheless CMOS detector allowed to evaluate glucose concentration in both normal and pathological conditions.

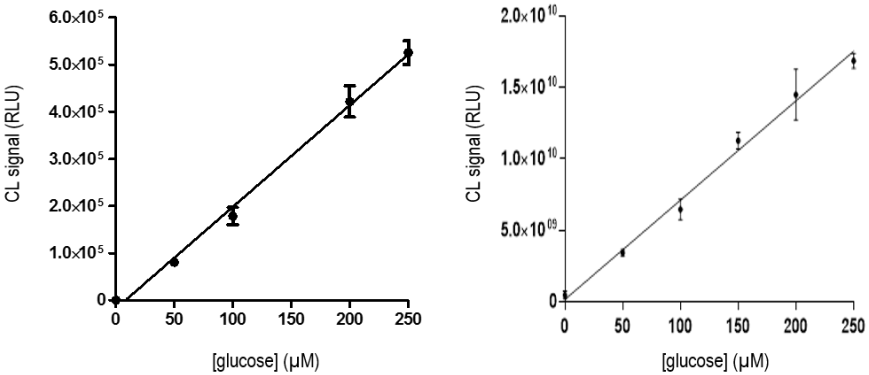

Figure 7.3 *Calibration curves of glucose, in the range of 50 – 250 µM, in carbonate 0,1 M buffer solution obtained using a CMOS sensor (on the left) and CCD camera (on the right). Each measurement is the average of three replicates.*

7.3. APPLICATION ON REAL SAMPLES: CALIBRATION CURVE IN HUMAN SERUM

In order to evaluate the applicability of the method to the analysis of real samples, calibration curve was generated by adding known concentration of glucose into human serum instead of carbonate buffer solution. This calibration curve was then compared to that obtained in buffer.

Preliminarily, the optimum dilution factor for the sample was established based on the nominal blood glucose values, which are between 3,9 and 6,1 mM. Considering this range of values, it was decided to dilute samples 1:50 (V/V) so that a sample with a maximum nominal blood glucose coincides to the half of the calibration curve. This dilution would thus allow to discriminate both hypoglycaemic and hyperglycaemic specimens.

The results obtained are shown in Figure 7.4. The equation obtained for the calibration curve in serum was $y = (2420 \pm 230)x + (339000 \pm 35000)$ and the linear correlation was $R^2 > 0,97$. The slope obtained for both calibration curves were similar (2160 ± 80 in buffer versus 2420 ± 230 in serum), as could be assumed, given that the high dilution of the sample should reduce the matrix effect. These preliminary results therefore suggest the applicability of the method for determining glucose content in serum (and presumably plasma) samples. Based on the results it is also concluded that the concentration of glucose of the used serum pool is just over 7.1 mM that is slightly over the physiological range.

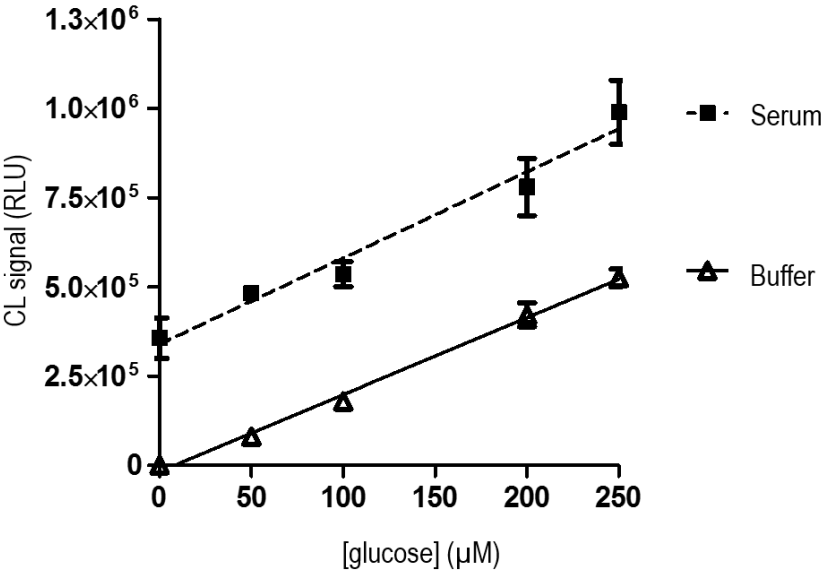

Figure 7.4 *Comparison between the calibration curve performed in carbonate 0,1 M buffer solution and the performed in serum 1:50 (V/V). Each measurement is the average of three replicates.*

8. CONCLUSIONS

As seen, the study was divided in two projects. The conclusion obtained for each one are:

1. Optimization of an immunoassay for ATP detection.

- The indirect competitive CL-based immunoassay, which consists in the competition between ATP present in the sample and immobilized ATP conjugated to ovalbumin for binding Anti-ATP antibody, was choosen as the most suitable immunological format after the assays in nitrocellulose.

- The immunoassay format choosen was correctly transferred to microplate format. After the optimization it was decided that proper incubation time was 1 h out of wells and the Anti-ATP antibody dilution chose was 1:5000.

- The CL immunoassay showed good analytical performances achieving high detectability (LOD: 0.01 nmol).

- The next step for this project will be the implementation of this immunoassay on a portable platform integrated with a-Si:H photosensors for the CL detection. The implementation of the CL bioassay into the compact and fully-integrated device will provide a new analytical platform for the multiparametric detection of bio-organic molecules outside of the Earth.

2. Paper-based device with chemiluminescent detection for glucose quantification in serum samples

- The adaptation of the device to the use of CMOS sensor for the detection was successfully achieved.

- CMOS sensor provides more compactness and portability than CCD camera without a significant loss in detectability. Moreover the use of CL as detection principle made it possible to achieve high sensitivity with a limit of detection of 30 μM of glucose.

- In the future this device could be adapted for the detection of different biomarkers and for multiplexed analysis. The high sensitivity and the simplicity of the system pave the way for a

new generation of analytical devices that can be easily used for a wide range of in-field and point-of-care bio-analyses.

9. REFERENCES AND NOTES

1. Aguilera-Herrador, E.; Cruz-Vera, M.; Valcárcel, M. Analytical connotations of point-of-care testing. Analyst. 2010, 135, 2220-2232.
2. Roda, A.; Guardigli, M. Analytical chemiluminescence and bioluminescence: latest achievements and new horizons. Anal. Bioanal. Chem. 2012, 402, 69-76.
3. Forster, R. J.; Bertoncello, P.; Keyes, T. E. Electrogenerated chemiluminescence. Annu. Rev. Anal. Chem. 2009, 2, 359-385.
4. Hummelen, J. C.; Luider, T. M.; Wynberg, H. Stable. 1,2-dioxetanes as labels for chemiluminescent immunoassay. Methods Enzymol. 1986, 133, 531−557.
5. Roda, A. Chemiluminescence and bioluminescence: Past, Present and Future. Royal Society Chemistry. 2011, 1st Edition
6. Mirasoli, M.; Guardigli, M.; Michelini, E.; Roda, A. Recent advancements in chemical luminescence-based lab-on-chip and microfluidic platforms for bioanalysis. Journal of Pharmaceutical and Biomedical Analysis. 2014, 87, 36-52.
7. Roda, A.; Pasini, P.; Guardigli, M.; Baraldini, M.; Musiani, M.; Mirasoli, M. Bio- and chemiluminescence in bioanalysis. J. Anal. Chem. 2000, 366, 752-759
8. Lengger, S.; Otto, J.; Elsässer, D.; Schneider, O.; Tiehm, A.; Fleischer, J.; Niessner, R.; Seidel, M. Oligonucleotide microarray chip for the quantification of MS2, ΦX174, and adenoviruses on the multiplex analysis platform MCR 3. Anal. Bioanal. Chem. 2014, 406, 3323-3334.
9. Zangheri, M.; Di Nardo, F.; Anfossi, L.; Giovannoli, C.; Baggiani, C.; Roda, A.; Mirasoli, M. A multiplex chemiluminescent biosensor for type B-fumonisins and aflatoxin B1 quantitative detection in maize flour. Analyst. 2015, 140, 358-365.
10. Zhou, Z.; Xu, L.; Wu, L.; Su, B. A novel biosensor array with a wheel-like pattern for glucose, lactate and choline based on electrochemiluminescence imaging. Analyst. 2014, 139, 4934-4939.
11. Singh, R.R.; Leng, L.; Guenther, A.; Genov, R. A CMOS-Microfluidic chemiluminescence contact imaging microsystem. IEEE Journal of Solid-State Circuits. 2012, 47, 2822-2833.
12. Rodrigues, E.R.G.O, Lapa, R.A.S. CMOS arrays as chemiluminescence detectors on microfluidic devices. Anal. Bioanal. Chem. 2010, 397, 381-388.
13. Tanaka, T.; Saeki, T.; Sunaga, Y.; Matsunaga, T. High content analysis of single cells directly assembled on CMOS sensor based on color imaging. Biosens. Bioelectron. 2010, 26, 1460-1465.
14. Mirasoli, M.; Nascetti, A.; Caputo, D.; Zangheri, M.; Scipinotti, R.; Cevenini, L.; de Cesare, G.; Roda, A. Multiwell cartridge with integrated array of amorphous silicon photosensors for chemiluminescence detection: development, characterization and comparison with cooled-CCD luminograph. Anal. Bioanal. Chem. 2014, 406, 5645–5656.
15. Gellman, S. H. Introduction: molecular recognition. Chem. Rev. 1997, 97, 1231-1232
16. Zhao, L.; Sun, L.; Chu, X. Chemiluminescence immunoassay. Trends Anal. Chem. 2009, 28, 404-415.
17. Marquette, C. A.; Blum, L.J. State of the art and recent advances in immunoanalytical systems. Biosens. Bioelectron. 2006, 21, 1424-1433.
18. Manz A.; Eijkel, J. C. T. Miniaturization and chip technology. What can we expect? Pure Appl. Chem. 2001, 73, 1555–1561.
19. Lion, N.; Reymond, F.; Girault, H. H.; Rossier, J. S. Why the move to microfluidics for protein analysis? Curr. Opin. Biotechnol. 2004, 15, 31–37.

20. Beebe, D. J.; Mensing, G. A.; Walker, G. M. Physics and applications of microfluidics in biology. Annu. Rev. Biomed. Eng. 2002, 4, 261–286.
21. Brody, J.; Yager, P.; Goldstein, R.; Austin, R. Biotechnology at low Reynolds numbers. Biophys. J. 1996, 71, 3430–3441.
22. Chin, C. D.; Linder, V.; Sia, S. K. Lab-on-a-chip devices for global health: past studies and future opportunities. Lab on a Chip. 2007, 7, 41–57.
23. Rossier, J. S.; Gokulrangan, G.; Girault, H. H.; Svojanovsky, S.; Wilson, G. S. Characterization of protein adsorption and immunosorption kinetics in photoablated polymer microchannels. Langmuir. 2000, 16, 8489–8494.
24. Goldstein, B.; Coombs, D., He, X.; Pineda, A. R.; Wofsy, C.; The influence of transport on the kinetics of binding to surface receptors: application to cells and BIAcore. J. Mol. Recognit. 1999, 12, 293–299.
25. Bange, A.; Halsall, H.B.; Heineman, W.R. Microfluidic immunosensor systems. Biosens. Bioelectron. 2005, 20, 2488-2503.
26. Nam Han, K.; Ai Li, C.; Hun Seong, G. Microfluidic chips for immunoassays. Annu. Rev. Anal. Chem. 2013, 6, 119-141.
27. Zimmermann, M.; Delamarche, E.; Wolf, M.; Hunziker, P. Modeling and optimization of high-sensitivity, low-volume microfluidic-based surface immunoassays. Biomed. Microdevices. 2005, 7, 99–110.
28. Apple, F.S.; Christenson, R.H.; Valdes, R.; Andriak, A.; Berg, A.; Duh, S.; Feng, Y.; Jortani, S.A.; Johnson, N.A.; Koplen, B.; Mascotti, K.; Wu, A.H.B. Simultaneous rapid measurement of whole blood myoglobin, creatine kinase MB, and cardiac troponin I by the triage cardiac panel for detection of myocardial infarction. Clin. Chem. 1999, 45, 199–205.
29. Mace, C. R.; Deraney, R. N. Manufacturing prototypes for paper-based diagnostic devices. Microfluid Nanofluid. 2014, 16, 801–809.
30. Carr, M. H. Water on Mars. Oxford University Press. 1996.
31. Mumma, M. J.; Villanueva, G. L.; Novak, R. E.; Hewagama, T.; Bonev, B. P.; DiSanti, M. A.; Mandell, A. M.; Smith, M. D. Strong release of methane on Mars in northern summer. Science. 2003, 323, 1041-1045.
32. Sims, M. R.; Cullen, D. C.; Rix, C. S.; Buckley, A.; Derveni, M.; Evans, D.; García-Con, L. M.; Rhodes, A.; Rato, C. C.; Stefinovic, M.; Sephton, M. A.; Court, R. W.; Bulloch, C.; Kitchingman, I.; Ali, Z.; Pullan, D.; Holt, J.; Blake, O.; Sykes, J.; Samara-Ratna, P.; Canali, M.; Borst, G.; Leeuwis, H.; Prak, A.; Norfini, A.; Geraci, E.; Tavanti, M.; Brucato, J.; Holm, N. Development status of the life marker chip instrument for ExoMars. Planetary and Space Science. 2012, 72, 129-137.
33. Parnell, J.; Cullen, D.; Sims, M. R.; Bowden, S.; Cockell, C. S.; Court, R.; Ehrenfreund, P.; Gaubert, F.; Grant, W.; Parro, V; Rohmer, M.; Sephton, M.; Stan-Lotter, H.; Steele, A.; Toporski, J.; Vago, J. Searching for Life on Mars: Selection of Molecular Targets for ESA's Aurora ExoMars Mission. Astrobiology. 2007, 7, 578-604.

.

10. ACRONYMS

POCT Point-of-care testing

CL Chemiluminescence

HRP Horseradish peroxidase

PMT Photomultiplier tube

CCD Charge-couple device

CMOS Complementary metal oxide semiconductors

IA Immunoassay

LOC Lab-on-chip

LMC Life marker chip

PLEIADES Planetary Life Explorer with Integrated Analytical Detection and Embedded Sensors

ATP Adenosine Triphosphate

GOx Glucose oxidase

BSA Bovine serum albumin

PBS Phosphate Buffered Saline

HRP-Biotin HRP conjugated to biotin

ATP-Biotin ATP conjugated to biotin

ATP-OVA ATP conjugated to Ovalbumin

ATP-BSA ATP conjugated to BSA

AntiRabbit-HRP Antibody AntiRabbit conjugated to HRP

AntiMouse-HRP Antibody AntiMouse conjugated to HRP